JNeurosci
THE JOURNAL OF NEUROSCIENCE

Research Articles: Systems/Circuits

Post-surgical latent pain sensitization is driven by descending serotonergic facilitation and masked by μ-opioid receptor constitutive activity (MOR_{CA}) in the rostral ventromedial medulla

https://doi.org/10.1523/JNEUROSCI.2038-21.2022

Cite as: J. Neurosci 2022; 10.1523/JNEUROSCI.2038-21.2022

Received: 9 October 2021
Revised: 22 May 2022
Accepted: 27 May 2022

Post-surgical latent pain sensitization is driven by descending serotonergic facilitation and masked by μ-opioid receptor constitutive activity (MOR_{CA}) in the rostral ventromedial medulla

Abbreviated title: Descending 5HT facilitation drives latent pain sensitization

Andrew H. Cooper[+,#], Naomi S. Hedden[+], Pranav Prasoon, Yanmei Qi, and Bradley K. Taylor[*]

Department of Anesthesiology and Perioperative Medicine, Pittsburgh Center for Pain Research, and the Pittsburgh Project to end Opioid Misuse, University of Pittsburgh School of Medicine, Pittsburgh, PA 15213 USA

[+]Co-first author

*Corresponding author: Brad Taylor, bkt@pitt.edu

Number of figures: 5

Number of words

Significance - 98/120; Abstract - 243/250; Introduction – 550/650; Discussion - 1529/1500

Conflict of interest statement: The authors declare no competing financial interests.

Acknowledgments: The authors thank Diogo da Silva dos Santos for his technical assistance. This work was supported by NIH grants R01DA037621, R01NS45954, R01NS62306 and R01NS112321 to BKT

[#]Current address: Institute of Neuroscience and Psychology, School of Medical, Veterinary and Life Sciences, University of Glasgow, Glasgow, G12 8QQ, UK

Abbreviations: CFA, complete Freund's adjuvant; CNO, clozapine N-oxide; CTAP, D-Phe-Cys-Tyr-D-Trp-Arg-Thr-Pen-Thr-NH2; DH, dorsal horn; DNIC, diffuse noxious inhibitory controls; DREADD, designer receptor exclusively activated by designer drugs; LS, latent sensitization; MOR, μ-opioid receptor; MOR_{CA}, μ-opioid receptor constitutive activity; NTX, naltrexone; PIM, plantar incision model; RVM, Rostroventral medial medulla; RMg, raphe magnus; RPa, raphe pallidus.

Abstract

Following tissue injury, latent sensitization (LS) of nociceptive signaling can persist indefinitely, kept in remission by compensatory μ-opioid receptor constitutive activity (MOR_{CA}) in the dorsal horn of the spinal cord. To demonstrate LS, we conducted plantar incision in mice and then waited 3-4 weeks for hypersensitivity to resolve. At this time (remission), systemic administration of the opioid receptor antagonist / inverse agonist naltrexone reinstated mechanical and heat hypersensitivity. We first tested the hypothesis that LS extends to serotonergic neurons in the rostral ventral medulla (RVM) that convey pronociceptive input to the spinal cord. We report that in male and female mice, hypersensitivity was accompanied by increased Fos expression in serotonergic neurons of the RVM, abolished upon chemogenetic inhibition of RVM 5-HT neurons, and blocked by intrathecal injection of the 5-HT_3R antagonist ondansetron; the 5-HT_{2A}R antagonist MDL-11,939 had no effect. Second, to test for MOR_{CA}, we microinjected the MOR inverse agonist CTAP and/or neutral opioid receptor antagonist 6β-naltrexol. Intra-RVM CTAP produced mechanical hypersensitivity at both hindpaws. 6β-naltrexol had no effect by itself, but blocked CTAP-induced hypersensitivity. This indicates that MOR_{CA}, rather than an opioid ligand-dependent mechanism, maintains LS in remission. We conclude that incision establishes LS in descending RVM 5-HT neurons that drives pronociceptive 5-HT_3R signaling in the dorsal horn, and this LS is tonically opposed by MOR_{CA} in the RVM. The 5-HT_3 receptor is a promising therapeutic target for the development of drugs to prevent the transition from acute to chronic post-surgical pain.

Significance statement

Surgery leads to latent pain sensitization and a compensatory state of endogenous pain control that is maintained long after tissue healing. Here we show that either chemogenetic inhibition of serotonergic neuron activity in the rostral ventromedial medulla (RVM), or pharmacological inhibition of 5-HT_3 receptor signaling at the spinal cord blocks behavioral signs of post-surgical latent sensitization. We conclude that μ-opioid receptor constitutive activity (MOR_{CA}) in the RVM opposes descending serotonergic facilitation of LS, and that the 5-HT_3 receptor is a promising therapeutic target for the development of drugs to prevent the transition from acute to chronic post-surgical pain.

INTRODUCTION

Chronic post-surgical pain impacts approximately 10% of patients and is often resistant to treatment (Glare et al., 2019). After an incision heals, a state of latent sensitization (LS) continues, whereby spinal nociceptive transmission in the dorsal horn (DH) remains within a state of heightened responsivity (Basu et al., 2021), kept in remission by compensatory signaling through inhibitory GPCRs including the neuropeptide Y Y1 receptor (Fu et al., 2019, 2020), kappa opioid receptor (Custodio-Patsey et al., 2020; Basu et al., 2021), and μ-opioid receptor (MOR) (Corder et al., 2013; Walwyn et al., 2016; Cooper et al., 2021). This endogenous analgesia lasts for long durations, in part due to MOR constitutive activity (MOR_{CA}). Even when delivered over a year after incision, administration of an opioid receptor antagonist or inverse agonist can "unmask" LS, precipitating a bilateral reinstatement of mechanical hypersensitivity and ongoing pain (Corder et al., 2013). The long duration of LS and MOR_{CA} could render studies in animal models particularly relevant to our understanding of the mechanisms that determine the initiation and maintenance of chronic post-surgical pain.

The ascending transmission of spinal nociceptive signals from the periphery to the brain are subject to powerful bulbospinal control. Supraspinal sites contribute to LS and MOR_{CA}, namely the central nucleus of the amygdala (CeA) (Cooper et al., 2021). However, the contribution of other brain areas remains unclear. Of particular interest is the rostral ventromedial medulla (RVM). Pain-modulatory signals from higher centers in the brain converge upon the RVM before descending to the DH (Porreca et al., 2002; Fields, 2004). Pathways from the RVM can be inhibitory or excitatory, and their net impact determines the modulation of spinal nociceptive signaling (Porreca et al., 2002; Fields, 2004; Chen and Heinricher, 2019). Tissue or nerve injury can shift this balance towards descending facilitation (Vera-Portocarrero et al., 2006; Bee and Dickenson, 2008; King et al., 2009; LaGraize et al., 2010; Wei et al., 2010; Wang et al., 2013). For example, in the setting of inflammation, disruption of pronociceptive signaling by MOR-expressing neurons in the RVM (RVM-MOR neurons) reduces inflammatory hyperalgesia (Kincaid et al., 2006; Cleary and Heinricher, 2013; Carr et al., 2014; Khasabov et al., 2017). RVM-MOR neurons likely mediate the well-known anti-hyperalgesic actions of exogenously administered morphine (Heinricher et al., 2009), but much less clear is their contribution to endogenous opioid receptor signaling such as MOR_{CA}.

RVM neurons that project to the dorsal horn include 5-HT cells within the raphe magus (Bowker et al., 1981; Skagerberg and Björklund, 1985). Optogenetic activation of medullary 5-HT neurons induced long-lasting mechanical and thermal hypersensitivity in uninjured mice (Cai et al., 2014), indicating their pronociceptive potential. This potential can be unleashed after nerve injury, with numerous studies suggesting that serotonin release from medullary raphe neurons targets spinal $5\text{-}HT_{2A}$ and $5\text{-}HT_3$ receptors to facilitate behavioral signs of

peripheral neuropathic pain (Suzuki et al., 2004; Steenwinckel et al., 2008; Thibault et al., 2008; Dogrul et al., 2009; Okubo et al., 2013; Kim et al., 2014; Bannister et al., 2015; Patel and Dickenson, 2018). In states of persistent inflammatory pain, however, the contribution of 5-HT_3R-mediated descending facilitation is unclear. Here we address these questions using chemogenetic and pharmacological approaches to target the activity of medullary 5-HT neurons, MOR_{CA} in the RVM and spinal 5-HT_3 receptors in a plantar incision model of latent pain sensitization.

MATERIALS and EXPERIMENTAL PROCEDURES

Animals

All procedures were approved by the University of Pittsburgh Institutional Animal Care and Use Committee in accordance with American Veterinary Medical Association and International Association for the Study of Pain guidelines. FEV^{cre} (mice that express Cre recombinase in mid/hindbrain serotonergic neurons; B6.Cg-Tg(Fev-cre)1Esd/J; stock #012712) (Scott et al., 2005) and Ai14 (mice that Cre-dependently express tdTomato; B6.Cg-*Gt(ROSA)26Sor*$^{tm14(CAG-tdTomato)Hze}$/J; stock #012712) (Madisen et al., 2010) mice were obtained from The Jackson Laboratory (ME, USA) and bred in our in-house colony. Male and female mice hemizygous for the FEV^{cre} transgene were used for chemogenetic behavioral experiments. For histology and *in situ* hybridization studies, FEV^{cre} mice were crossed with Ai14 mice. Wild-type C57BL/6 (used for all other behavioral pharmacology) and CD1 (used for all other histology) mice were obtained from Charles River Laboratories (MA, USA). Mice aged 6-16 weeks at the beginning of experiments were housed 2-4 per cage and maintained on a 12/12 light/dark cycle at 20-22°C and 45 ± 10% relative humidity, with food and water provided *ad libitum.* Mice were handled and habituated to testing equipment for 30 min/day for 3 consecutive days prior to experimental manipulations and all procedures were performed during the animals' light cycle (between 7am and 7pm).

Viruses

For chemogenetic experiments, we used a control reporter virus that induced Cre-dependent expression of the fluorescent protein mCherry, AAV2-hSyn-DIO-mCherry (Addgene viral prep # 50459-AAV2; RRID: Addgene_50459; lot # v54505; 1.8×10^{13} vg/mL) or an experimental virus designed to express a neuron-specific, inhibitory G-coupled DREADD, AAV2-hSyn-DIO-hM4D(G_i)-mCherry (Addgene viral prep # 44362-AAV2, RRID: Addgene 44362; lot # v68359; 1.5×10^{13} vg/mL, a gift from Bryan Roth (Krashes et al., 2011)). As described below, either control or experimental virus were targeted to the RVM of FEV^{cre} mice to generate $RVM^{FEV\text{-}mCherry}$ or $RVM^{FEV\text{-}hM4Di)}$ mice, respectively. Viruses were stored in 5 µL aliquots at -80°C and thawed on ice immediately prior to injection.

Plantar incision model (PIM) of post-surgical pain

Plantar incision was performed as previously described (Pogatzki and Raja, 2003; Basu et al., 2021). Anesthesia was induced with 5% isoflurane (Abbott Laboratories, USA) and then maintained at 2% isoflurane. Ophthalmic ointment was applied to the eyes and plantar skin was swabbed with chlorhexidine solution (Chloraprep, BD Healthcare, USA). A 4-mm midline, longitudinal incision was made through the glabrous skin of the left hindpaw, from the interdigital pads to the heel. The plantaris muscle was separated from underlying tissue and then a 4-mm midline longitudinal incision was made through the muscle with a #11 scalpel blade. The skin incision was closed with two 5-0 PDSII (polydioxanone) sutures (Ethicon), followed by topical application of Neosporin ointment (Johnson and Johnson, USA). Sham-operated mice received isoflurane for the same duration as PIM-operated mice but no incisions were made.

Stereotaxic surgery

Mice received carprofen (2 mg chewable tablet per mouse, per day, 24 hours prior to surgery and for 2 days after; Bio-Serv, USA) and a peri-operative injection of buprenorphine (0.1 mg/kg, subcutaneous; Covetrus, USA). Surgical anesthesia was induced with 5% isoflurane and maintained at 2% isoflurane. Mice were placed in a stereotaxic apparatus fitted with blunt mouse ear bars (Stoelting, USA). Ophthalmic ointment (Fisher Scientific, USA) was applied to the eyes, the scalp was shaved, and skin was swabbed with chlorhexidine solution. A midline skin incision exposed the cranium and with a 0.7 mm dental burr bit, a hole was drilled (World Precision Instruments, USA) above the nucleus raphe magnus (RMg) of the RVM (coordinates relative to bregma: -5.8 to 6 mm AP; 0 mm ML; -5.6 mm DV), according to Paxinos and Franklin (2013). Mice were housed in pairs for a recovery period of at least 6 to 8 days prior to further experimental manipulations.

Cannulation surgeries were performed two weeks after incision and one to two weeks prior to behavioral pharmacology. A 26 Ga, 4.6 mm stainless steel guide cannula (cat # C315G-SPC, PlasticsOne, USA) was implanted 1 mm above the RMg. The guide cannula was affixed to the skull with two flat-head jeweler's screws (0-80 x 1/8", Small Parts, USA) and dental cement (RelyX Luting Plus Automix, 3M, USA). Skin was then closed around the base of the cannula using three 5-0 PDSII suture (Ethicon, USA), followed by insertion of a 4.6 mm stylet (cat # C315DC-SPC, PlasticsOne, USA) into the guide cannula to prevent clogging.

AAV microinjections were performed one week prior to incision. A 33-gauge needle (PlasticsOne, USA) attached to a 1 µL microsyringe (Hamilton, USA) with PE-50 tubing (Warner Instruments, CT, USA) was inserted slowly into the RMg (-5.6 mm DV) over 5 minutes. 300 nL of AAV were then slowly injected over 5 minutes. The needle left in place for a further 5-10 minutes to prevent backflow of solution up the needle tract, and then slowly

retracted over a period of 5 minutes. Skin was then closed using three 5-0 PDSII sutures and cyanoacrylate glue (Vetbond; 3M, USA).

Drug administration and experimental design

Intra-cranial drug infusion

Injections were performed using a 33-gauge injection cannula (cat # C315I-SPC, PlasticsOne, USA) that extended 1 mm beyond the tip of the guide cannula. The injection cannula was attached to flexible plastic tubing (cat # C313C, PlasticsOne, USA), backfilled with mineral oil, and connected to a microliter syringe (Hamilton, USA). D-Phe-Cys-Tyr-D-Trp-Arg-Thr-Pen-Thr-NH2 (CTAP, 0.3 µg/0.25 µL; Tocris, UK), a MOR-selective inverse agonist was dissolved in sterile saline. 6β-naltrexol hydrate (3 µg/0.25 µL; Sigma-Aldrich, USA, most often described as a neutral opioid receptor antagonist (Raehal, 2005; Sirohi et al., 2009; Lam et al., 2011)) was dissolved in 10% DMSO in sterile saline. Reports claiming 6β-naltrexol to be an inverse agonist (Sally et al., 2010) were based on recombinant MOR over-expression assays in cell lines and may not recapitulate neutral antagonist activity as occurs in vivo. Drugs were slowly infused using a syringe pump (Harvard Apparatus, USA) at a volume of 0.25 µL over 6 minutes. The injection cannula was left in place for a further 15 minutes to prevent backflow. Successful microinjection was confirmed by movement of a small air bubble within the mineral oil along the tubing. CTAP dose was based on our previous data using the intra-cranial route of administration (Cooper et al., 2021), and 6β-naltrexol dose was based upon the molar ratio of CTOP: 6β-naltrexol required to inhibit reinstatement of mechanical hypersensitivity via the intrathecal route (10:1) (Corder et al., 2013). 21 days after incision, the first intra-RVM microinjection of drug or vehicle was conducted and this was followed 7 days later with a crossover injection of vehicle or drug.

Intrathecal injection

A small patch of fur (~20 x 20 mm) was shaved over the lumber spine. Mice were acclimated to manual restraint at the pelvic girdle within a towel to minimize stress. After insertion of a 30-G needle (attached to a 25 µL Hamilton syringe) between the L5 and L6 vertebrae, successful entry was indicated by observation of a tail flick (2/135 injections were excluded). Drug or its vehicle (5 µL) were slowly injected over 20 seconds into the intrathecal space and then the needle was held in place for an additional 10 seconds to minimize backflow (Njoo et al., 2014). The 5-HT_3R antagonist ondansetron (Tocris, UK) or 5-HT_{2A}R antagonist MDL-11,939 (Tocris, UK) were dissolved in saline or 0.68% DMSO in saline, respectively. Dosages were selected based on previous literature using the intrathecal route of administration (Pehek et al., 2006; Thibault et al., 2008; Van Steenwinckel et al., 2008; Chang et al., 2013).

Systemic injection for chemogenetics

Clozapine N-oxide (CNO, Tocris, UK) was dissolved in sterile saline at a dose of 3 mg/kg to achieve hM4D activation (Peirs et al., 2015) while minimizing clozapine-mediated adverse effects (Manvich et al., 2018). Mice were randomly allocated to one of 4 treatment groups (CNO or vehicle, intraperitoneal; NTX or vehicle, subcutaneous at nape). 21 days after incision, mice received CNO or its saline vehicle injection followed 5 minutes later with naltrexone or vehicle, and then tested for mechanical sensitivity. This was followed 7 days later with a crossover injection of vehicle or naltrexone. To the same mice, 35 days later, injections were followed by assessment of heat hypersensitivity and then tested 5 days later with a crossover design.

Behavioral testing

All behavioral measurements were performed by an investigator blinded to experimental treatments by an assistant who randomly assigned treatment groups.

Von Frey assessment of mechanical allodynia

Hindpaw 50% mechanical withdrawal thresholds were measured with a predefined set of 8 von Frey (vF) monofilaments (0.008 to 6 g, Stoelting, Inc, IL, USA) using the up-down method (Chaplan et al., 1994). Mice were acclimated for at least 15 minutes within an acrylic box, opaque on all sides, atop an elevated wire mesh platform. The vF hair was applied to the proximal region of the glabrous skin at the plantar surface of the hindpaw, just lateral to the incision site. Each trial began with application of an intermediate filament (0.16 g), perpendicular to the skin, causing a slight bending, for 3 seconds. In case of a positive response (rapid withdrawal or licking of the paw within 3 seconds of removing of the filament, but ignoring normal ambulation or rearing), the next smallest filament was tested. In case of a negative response, the next larger filament was tested. Each trial continued until 4 measurements beyond the first change in response (i.e., no response then response, or vice versa) were taken. 50% mechanical withdrawal threshold was calculated using the statistical method described by Dixon (1965).

Plantar radiant heat assay (Hargreaves test)

Heat sensitivity was assessed with a radiant heat assay (Ugo Basile, Italy). Up to 7 mice were tested at a time on an elevated glass platform within 7”H x 15”W x 35”L acrylic boxes, transparent on one side to enable the experimenter to observe from the front. Following at least 25 minutes of acclimation, a radiant heat source was applied through the glass floor to the plantar surface of the hindpaw (Hargreaves et al., 1988). Latency to paw withdrawal was recorded, ignoring normal ambulation. Thermal stimulation was applied for no longer than 20 seconds to avoid tissue damage. Withdrawal latency was measured 3 times at 5-min intervals (5-min before, 0 and 5-min after the defined timepoint) and averaged.

Hotplate test

For chemogenetic studies, hotplate testing was used as an alternative assay of heat hypersensitivity because our pilot studies found that CNO induced a small, DREADD-independent change in thermoregulation when mice were in contact with the glass platform for extended periods of time. Mice were placed on a hotplate (Columbus Instruments, USA) at 52.5°C, and the latency to response (jumping, licking, or rapid withdrawal) at either hindpaw was recorded. At this time, mice were returned to their home cage. Withdrawal latency was measured 3 times at 10-min intervals (10-min before, 0 and 10-min after the defined timepoint) and averaged.

Histology

Confirmation of cannulation sites

After completion of intra-RVM behavioral pharmacology experiments, mice were anesthetized with an overdose of pentobarbital (5 mL/kg, i.p.; Fatal Plus, Vortech Pharmaceuticals, USA), perfused with 4% paraformaldehyde (PFA; Sigma Aldrich, USA), and then received an intra-RVM microinjection of 0.25 µL India ink. After 15 minutes for dye penetration, brains were removed, postfixed in 4% PFA at 4°C overnight, cryoprotected in 30% sucrose for a further 48 hours, and then embedded in optimal cutting temperature media (OCT; Tissue Tek, Andwin Scientific, USA). Brains were sectioned on a cryostat (Cryostar NX70, Fisher Scientific, USA) at 30 µm, collected on gelatinized slides, counterstained with Cresyl violet, and then imaged. The location of staining was cross-referenced with a stereotaxic atlas (Paxinos and Franklin, 2013) to confirm injection site. In all mice, the center of cannula placements was found to be within 0.2 mm from the outer boundary of the RMg, with India ink spreading into the RMg, and so all were considered to have been on-target.

Fos immunohistochemistry

21 days after incision or sham surgery, mice were transcardially perfused with 4% PFA. Brains were collected, embedded in OCT and sectioned on the cryostat at 40 µm coronal cryosections. Free-floating sections were collected 0.1 M PBS. Six non-adjacent, evenly spaced sections spanning the range between Bregma -5.6 to -6.2 mm (Paxinos and Franklin, 2013) were arbitrarily selected from each mouse. Sections were washed in PBS, then blocked in PBS containing 3% normal goat serum (NGS; MP Biomedicals) and 0.3% Triton X-100 (VWR, USA) for 1 hour, and then incubated for 18 hours at room temperature with either anti-Fos (1:2000; polyclonal rabbit anti-cFos; Synaptic Systems, Germany; Cat# 226 003, RRID:AB_2231974) and anti-NeuN (1:1000; Alexa Fluor-488-conjugated mouse anti-NeuN; Millipore-Sigma, USA; Cat# MAB377X, RRID:AB_2149209), or anti-Fos (1:2000; rabbit anti-phospho-c-Fos (Ser32); Cell Signaling Technology, USA; Cat# 5348, RRID: AB_10557109), diluted in 1% NGS and 0.3% Triton X-100. Following further washes in PBS, slides were air-dried and coverslipped with Vectashield Hard Set Antifade Mounting Medium (Vector Labs, CA, USA).

Fluorescence in situ hybridization (FISH)

FEV^{cre}::Ai14 mice were administered an overdose of pentobarbital. Upon cessation of heartbeat, brains were rapidly extracted, embedded in OCT and frozen on dry ice. Brains were cryosectioned on a cryostat at 8 µm and mounted directly onto slides (Superfrost Plus, Fisher Scientific). Sections were fixed by immersion of slides in ice cold 4% PFA for 15 minutes and then dehydrated with increasing concentrations of ethanol (50%, 70% then 100% for 5 min each). Fluorescence *in situ* hybridization was performed using an RNAscope Multiplex Fluorescent Reagent Kit v2 (Advanced Cell Diagnostics, USA; Cat# 323100) following the manufacturer's protocol. Slides were pretreated for 15 minutes with protease (Advanced Cell Diagnostics, USA), and then incubated and hybridized with *Oprm1* mRNA probe (Cat. # 315841) for 2 hours at 40° C in a humidified oven (HybEZ; Advanced Cell Diagnostics, USA). Sections were incubated with 3 drops each of AMP1, AMP2, AMP3 then AMP4-FL amplification buffers for 30 min, 15 min, 30 min and 15 min respectively at 40° C, with 2 min rinses in wash buffer after each incubation. Slides were then washed in 0.01 M PBS, air-dried and coverslipped with Vectashield Hard Set Antifade Mounting Medium with DAPI (Vector Labs, CA, USA).

Imaging

Sections throughout the medullary raphe magnus (RMg) and raphe pallidus (RPa) were imaged with a Nikon Ti2 inverted epifluorescence microscope equipped with a motorized stage, 10x, 0.45 NA (used for brightfield confirmation of cannulation sites), 20x, 0.75 NA (used for Fos immunohistochemistry) and 40x, 0.95 NA (used for FISH) objectives, and a Prime BSI camera (Photometrics, USA). The same exposure time (80 to 500 ms) was used for all images captured in each channel. For Fos immunohistochemistry performed on FEVcre::Ai14 tissue, 10 to 12 z-scans (3 µm separation) of a field of view containing the RVM were acquired. Image capture, stitching and quantification were performed with NIS Elements Advanced Research software v5.02 (Nikon, Japan). Quantification of staining was conducted in the RMg and RPa. Anatomical landmarks and rostrocaudal coordinates (from bregma -5.6 to -6.2 mm) were referenced to a mouse brain atlas (Paxinos and Franklin, 2013). Throughout image acquisition and quantification, the investigator, while blind to treatment groups, adjusted brightness and contrast in the same manner for each image.

Quantification

The number of Fos-positive cell profiles were manually quantified in 4-8 mice per experimental group, excluding profiles that were largely outside of the plane of view, clearly not representing a soma, or with fluorescence that is readily attributed to artifacts. For each section, a minimum fluorescence intensity was established by examining brainstem nuclei outside of the RVM. Profiles with intensity below this threshold likely represented background/non-specific immunostaining and so were not counted. Fos and tdTomato colocalization was

quantified within z-stacks by scrolling back and forth in the z dimension to determine the z position with optimal focus, and to determine whether fluorescence in each channel occurred in the same focal plane. A positive cell was defined as a Fos+ nucleus surrounded by a tdTomato+ soma in x, y and z dimensions. To account for over-sampling of Fos+ neuronal profiles in the z-axis, a correction factor was calculated using Abercrombie's formula (ratio of "real" number to observed number = T/T + h, where T is section thickness and h is mean diameter of objects) (Guillery, 2002). Given a section thickness of 40 µm, a mean Fos+ neuronal nuclei diameter of 8.72 µm (determined by measuring diameter of all Fos+ nuclei in 3 randomly selected sections from our dataset), a correction factor of 0.82 was applied to all cell counts. 5 to 6 sections per mouse were counted and averaged, with *n* defined as 1 mouse. For quantification of FISH, an *Oprm1* positive cell was identified by a minimum of 4 fluorescent puncta within the soma surrounding the nucleus (Snyder et al., 2018).

Statistical analyses

Statistical analyses were performed in Prism 8.1 (GraphPad Software Inc., USA). Immunohistochemical data were compared with unpaired T-tests. Behavioral data were analyzed using two-way repeated measures (RM) ANOVA, examining the interaction of Treatment (incision or sham, and combinations of drugs or vehicle) and Time, unless otherwise specified. If ANOVA revealed a main effect, then Bonferroni post-hoc tests were conducted to compare between treatment groups. The threshold for statistical significance was set at $P < 0.05$. For immunohistochemical studies of Fig 2, *n* represents a single mouse. All behavioral and immunohistochemical results are presented as mean ± SEM.

RESULTS

3.1 MOR constitutive activity (MOR_{CA}) in the RVM maintains LS in remission.

Plantar incision produces mechanical hyperalgesia that peaks within 1-2 days and then gradually resolves over 14-21 days. At this point, latent sensitization (LS) is in a state of remission that is maintained by ongoing signaling from μ-opioid receptors in the dorsal horn (Corder et al., 2013) and amygdala (Cooper et al., 2021); however, the identity of additional critical brain regions remains a key gap in knowledge. An important supraspinal site in the regulation of chronic inflammatory pain is the RVM (Porreca et al., 2002). The experiments of Figure 1 investigated whether injury recruits MOR signaling in the RVM to maintain LS in remission. 14 days after incision, cannulae were inserted into the RVM of male mice (Fig. 1A-B). Incision but not sham surgery evoked a mechanical hypersensitivity that peaked at 2 days and resolved within 21 days (Fig. 1C). 21 days after surgery, mice received an intra-RVM microinjection of the MOR inverse agonist CTAP (0.3 μg/0.25 μL) or vehicle (saline). Intra-RVM CTAP but not saline reinstated mechanical hypersensitivity in incision but not sham mice (Time x Treatment interaction $F_{15,120} = 1.861$, $P = 0.039$; $n = 7$).

To determine whether ligand-dependent or ligand-independent opioid signaling in the RVM maintains LS in remission, we injected either CTAP (0.3 μg/0.25 μL), the neutral opioid antagonist 6β-naltrexol (3 μg/0.25 μL), a combination of both, or vehicle (10% DMSO in saline) into the RVM. Mechanical sensitivity was assessed at both hindpaws. As illustrated in Fig. 1D-E, incision induced a mechanical hypersensitivity in the ipsilateral but not contralateral hindpaw that resolved within 21 days (Time x Side interaction $F_{4,120} = 35.39$, $P < 0.001$; $n = 16$). When these animals were injected on post-surgical Day 21, CTAP but not saline reinstated mechanical hypersensitivity at the ipsilateral hindpaw (Fig. 1D, *right*) and produced robust hypersensitivity on the contralateral hindpaw as well (Fig. 1E). 6β-naltrexol had no effect when injected alone, indicating that latent sensitization is not suppressed by *ligand-dependent* MOR signaling in the RVM. By contrast, 6β-naltrexol blocked the hypersensitivity produced by CTAP (ipsilateral: Time x Treatment interaction $F_{15,140} = 2.964$, $P < 0.001$; contralateral: Time x Treatment interaction $F_{4,120} = 2.182$, $P < 0.001$; $n = 8$), indicating that latent sensitization is suppressed by ligand-independent MOR_{CA}.

3.2 Increased Fos expression in medullary raphe 5-HT neurons during NTX-induced reinstatement of hyperalgesia.

Transient application of noxious heat alters the firing of RVM neurons (Heinricher et al., 1989), and persistent chemical nociception evokes neurotransmitter release in the RVM (Taylor and Basbaum, 1995). Furthermore, the complete Freund's adjuvant (CFA) model of inflammatory pain is associated with facilitation of neuronal activity in the RVM (Ren and Dubner, 2002; Heinricher, 2016); however, these experiments were limited to the

initial stages of inflammation, typically 1-3 days after induction. To test the hypothesis that incision can produce a longer-lasting neuronal sensitization that is more reflective of the time course of chronic pain, we waited 21 days after incision and then assessed Fos expression as a marker of neuronal activity (Bullitt, 1990) as illustrated in Figure 2. Fig. 2A and Extended Data 2-1A illustrate that Fos was colocalized with neuronal nuclei marker NeuN. The number of Fos positive neurons increased after incision as compared with sham surgery (Fig. 2B Unpaired t-test; $t_{14} = 2.66$, $P = 0.019$; $n = 8$), indicating a long-lasting increase in RVM neuron activation.

Descending serotonergic facilitation arising from the RVM drives chronic neuropathic pain states (Suzuki et al., 2004; Dogrul et al., 2009; Kim et al., 2014; Bannister et al., 2015; Patel and Dickenson, 2018). To test the hypotheses that serotonergic neurons are activated during reinstatement of hypersensitivity, we examined Fos expression in the medullary raphe (RMg and RPa) of FEV^{cre}::Ai14 mice (Fig. 2C and Extended Data 2-1B). 21 days after incision, mice received a s.c. injection of NTX (3mg/kg) or vehicle (saline) and were then allowed a 2-hr waiting period to allow Fos expression. NTX increased Fos in serotonergic (FEV-tdTomato+) neurons compared to mice that received saline (Fig. 2D; Unpaired t-test; $t_6 = 5.301$, $P = 0.002$; $n = 8$).

The immunohistochemical evidence for co-expression of MOR and 5-HT in the RVM is contradictory (Gao and Mason, 2000; Sikandar et al., 2012). To re-address this question, we conducted fluorescence *in situ* hybridization (FISH) for *Oprm1* mRNA in the RMg and RPa of FEV^{cre}::Ai14 mice. Fig. 2E-F illustrate that 58.0 ± 3.7% FEV-tdTomato+ neurons expressed *Oprm1* mRNA, and 50.7 ± 4.6% *Oprm1*+ neurons expressed FEV-tdTomato. As a positive control, we also examined *Oprm1* mRNA expression in the spinal cord. As illustrated in Fig. 2G, *Oprm1* mRNA was particularly enriched in the superficial laminae as previously described (Wang et al., 2021). These data support the feasibility of serotonergic neurons as a target for inhibition by MOR_{CA}.

3.3 Chemogenetic inhibition of RVM 5-HT neurons prevents NTX-induced reinstatement of hyperalgesia.

Focal lesioning and local anesthesia studies suggest that descending facilitation arising from the RVM contributes to early hypersensitivity upon cutaneous inflammation (Urban et al., 1996; Kincaid et al., 2006; Tillu et al., 2008; Carr et al., 2014). However, interpretations of these studies can be confounded by disruption of axons of passage or compensatory changes. Further, these studies did not examine the contribution of RVM 5-HT neurons in a model of long-lasting inflammatory pain. To address these gaps, we chose chemogenetics in our incision LS model as an approach to selectively inhibit RVM 5-HT neurons with temporal control (Figure 3). As illustrated by the timeline in Fig. 3A, we injected a Cre-dependent virus expressing either the inhibitory DREADD hM4Di (AAV2-hSyn-DIO-hM4D(Gi)-mCherry) or a control virus expressing mCherry (AAV2-hSyn-DIO-mCherry) into the RVM of FEV^{cre} mice. Fig. 3B confirmed that hM4D-mCherry expression was largely restricted to RVM 5-HT (Tph2+) neurons: 87.16 ± 3.96% of hM4D-mCherry expressing neurons co-labelled with Tph2

immunofluorescence (*n* = 4 mice). One week after virus injection, we conducted incision or sham surgery. 21 days later, we first administered clozapine-*N*-oxide (CNO; 3 mg/kg, i.p.), and then challenged the mice with either NTX (3 mg/kg, s.c.) or vehicle (saline). As illustrated in Figure 3C and 3E, incision-induced mechanical and heat hypersensitivity at the ipsilateral hindpaw resolved within 21 days (mechanical: Time x Incision interaction, $F_{20,176} = 13.81$, $P < 0.001$; heat: Time x Incision interaction, $F_{4,44} = 28.22$, $P < 0.001$; n = 8 (sham) or 12 (PIM) $RVM^{FEV\text{-}hM4Di}$ and 5 $RVM^{FEV\text{-}mCherry}$ controls). CNO but not its vehicle abolished NTX-induced reinstatement of mechanical hypersensitivity at the ipsilateral paw of mice with incision but not in: 1) sham-operated mice; 2) those that received intra-RVM injection of mCherry control virus; nor 3) mice that did not receive NTX (*ipsilateral:* Fig. 3D; Time x Treatment interaction, $F_{25,190} = 6.074$, $P < 0.001$; *contralateral:* Fig. 3E; Time x Treatment interaction, $F_{25,190} = 7.682$, $P < 0.001$; Time x Treatment interaction, $F_{5,37} = 21.46$, $P < 0.001$; *both:* n = 7-8 $RVM^{FEV\text{-}hM4Di}$, 5 $RVM^{FEV\text{-}mCherry}$ controls). These data demonstrate that RVM 5-HT neurons maintain LS.

3.4 Spinal 5-HT_3 but not 5-HT_{2A} receptors contribute to latent sensitization.

Both 5-HT_{2A} and 5-HT_3 receptors contribute to descending serotonergic facilitation of spinal nociceptive signaling and the maintenance of the early stages of injury-induced hyperalgesia (Dogrul et al., 2009; Alba-Delgado et al., 2018; Patel and Dickenson, 2018); here, we determined the contribution of these receptors to longer-lasting hyperalgesia (Figure 4). As illustrated by the timeline of Fig. 4A, we conducted incision or sham surgery and then waited 21-28 days for remission. Incision produced mechanical and heat hypersensitivity at the ipsilateral paw that resolved within 21 days (Fig. 4B, *mechanical*: Time x Incision interaction, $F_{4,84} = 26.31$, $P < 0.001$, n = 9 (sham) or 14 (PIM); Fig. 4D, *heat*: Time x Incision interaction, $F_{2,44} = 46.49$, $P < 0.001$, n = 8 (sham) or 16 (PIM); Fig. 4E, *mechanical:* Time x Incision interaction, $F_{4,112} = 41.29$, $P < 0.001$, n = 15; Fig. 4G, *heat*: Time x Incision interaction, $F_{2,54} = 51.67$, $P < 0.001$, n = 9 (sham) or 20 (PIM)). We then intrathecally administered the 5-HT_3R antagonist ondansetron (10 µg/5 µl) or its vehicle (saline), and in a separate study, the 5-HT_{2A}R antagonist MDL-11,939 (0.5 µg/5 µl) or its vehicle (0.68% DMSO in saline). Five minutes later, we injected NTX (3 mg/kg, s.c.) or vehicle (saline). As illustrated in Figs. 4B-D, NTX led to the reinstatement of mechanical and heat hypersensitivity at the ipsilateral hindpaw, as well as contralateral mechanical hypersensitivity.

Ondansetron: 2-way RM ANOVA with Bonferroni post-tests revealed that ondansetron blocked NTX-induced reinstatement of mechanical hypersensitivity at the ipsilateral paw (Time x Treatment interaction, $F_{20,160} = 2.39$, $P = 0.001$, n = 6-8, Fig. 4B) and the contralateral paw (Time x Treatment interaction, $F_{20,160} = 2.45$, $P = 0.001$, n = 6-8, Fig. 4C) as well as heat hypersensitivity (Time x Treatment interaction, $F_{16,100} = 5.42$, $P < 0.001$, n = 6, Fig. 4D). Ondansetron did not change sensitivity in sham-operated mice nor in PIM mice that received saline vehicle.

MDL-11,939: In contrast to ondansetron, MDL-11,939 did not change NTX-induced reinstatement of mechanical hypersensitivity at the ipsilateral paw (Time x Treatment interaction, $F_{20,175} = 11.46$, $P < 0.001$, $n = 8$; Bonferroni post-tests comparing PIM + NTX + Sal and PIM + NTX + MDL: $P > 0.9$ at all timepoints; Fig. 4E), the contralateral paw (Time x Treatment interaction, $F_{20,175} = 6.88$, $P < 0.001$, $n = 8$; Bonferroni post-tests comparing PIM + NTX + Sal and PIM + NTX + MDL: $P > 0.9$ at all timepoints; Fig. 4F), nor heat hypersensitivity (Time x Treatment interaction, $F_{16,92} = 3.43$, $P < 0.001$, $n = 5$-7; Bonferroni post-tests comparing PIM + NTX + Sal and PIM + NTX + MDL: $P > 0.2$ at all timepoints; Fig. 4F).

DISCUSSION

Incision produces a long-lasting latent sensitization of RVM 5-HT neurons

Our study is the first to examine the activity of RVM neurons three weeks after surgery, during the remission phase of LS. We found that the number of RVM neurons expressing Fos was greater in PIM mice than in sham controls, suggestive of a tonic increase in activity, even in the absence of overt pain-like behavior. Furthermore, we observed greater Fos expression in FEV-tdTomato-positive neurons during NTX-induced reinstatement of hyperalgesia, leading us to conclude that incision produces a long-lasting latent sensitization of RVM 5-HT neurons. These results in our LS model of chronic postoperative pain extend previous studies that had been restricted to noxious stimulus-evoked responses in uninjured animals or in short-term models of persistent pain hypersensitivity (Heinricher, 2016).

The RVM contains three classes of neurons based on their electrophysiological responses to transient noxious stimuli: ON cells are pronociceptive MOR-expressing RVM neurons and display an increase in firing rate before or at the onset of nocifensive behaviors; OFF cells display a transient pause in firing; and neutral cells display no change in firing rate (Fields et al., 1983; Chen and Heinricher, 2019). Since the original hypothesis that MOR and 5-HT provided molecular identification of the ON-cell and neutral cell populations, respectively (Fields, 1992; Potrebic et al., 1994; Gao and Mason, 2000), more recent studies have suggested a more heterogenous distribution (Sikandar et al., 2012). Given that cre expression in FEV^{cre} mice faithfully recapitulates hindbrain serotonergic neuron populations (Scott et al., 2005), and the molecular identity of ON-cells includes expression of MOR (Heinricher et al., 1992), our finding that over 50% of *Oprm1*-expressing profiles co-express FEV-tdTomato supports the idea that 5-HT RVM neurons represent not only neutral cells but also a subpopulation of MOR-expressing ON-cells. Further studies are needed to determine whether increased neuronal activity reflects an engagement of LS mechanisms in molecularly-defined ON, OFF, and neutral cells.

RVM 5-HT neurons maintain the LS that is masked by endogenous opioid receptor activity

We found that chemogenetic silencing of RVM 5-HT neurons prevented NTX-induced reinstatement of mechanical and heat hypersensitivity in our LS model of chronic postoperative pain. These results are consistent with and extend the work of Carr et al, who reported that ablation of descending CNS serotonergic neurons with intrathecal 5,7-dihydroxytryptamine partially reduced mechanical hypersensitivity at early timepoints following ankle injection of CFA (Carr et al., 2014); in contrast to this study, we observed complete inhibition of mechanical hypersensitivity at much later timepoints in a model that more closely mimics the time course of chronic pain. We conclude that RVM 5-HT neurons maintain the LS that is masked by endogenous opioid receptor activity.

Optogenetic activation of RVM 5-HT neurons induces mechanical and thermal hypersensitivity in uninjured mice (Cai et al., 2014). By contrast, our control experiments revealed that chemogenetic inhibition by itself did not increase mechanical or heat hypersensitivity. This indicates that RVM 5-HT neurons do not exert tonic pain inhibition, including during the remission phase of LS.

Spinal 5-HT_3 receptors contribute to latent sensitization of post-surgical pain.

We show for the first time that intrathecal injection of the 5-HT_3R antagonist ondansetron blocked NTX-induced reinstatement of both mechanical and heat hypersensitivity when tested three weeks after plantar incision. We conclude that spinal 5-HT_3 receptors contribute to latent sensitization of post-surgical pain. This extends what has previously been observed in rodent models of neuropathic pain, where intrathecal ondansetron reduced the mechanical and thermal hypersensitivity and sensitization of dorsal horn neurons following peripheral nerve injury (Suzuki et al., 2004; Dogrul et al., 2009; Kim et al., 2014; Bannister et al., 2015; Patel and Dickenson, 2018). Furthermore, interruption of 5-HT_3R signaling with either global 5-HT_3R knockout (Zeitz et al., 2002) or shRNA interference of tryptophan hydroxylase-2 (Wei et al., 2010) reduced licking behavior and/or dorsal horn neuronal firing in the intraplantar formalin test. On the other hand, Dickenson and colleagues reported no effect of ondansetron in the intraplantar carrageenan model of early inflammatory pain (Rahman et al., 2004), and so it appears that spinal 5-HT_3 receptors maintain neuropathic pain, acute ongoing pain and long-lasting post-surgical pain, but not short-term inflammatory pain.

Ondansetron blocked NTX-induced reinstatement of hypersensitivity at both hindpaws, ipsilateral and contralateral to unilateral plantar incision. This is consistent with the idea that 5-HT_3R signaling contributes to mirror image pain. Similarly, ondansetron restored diffuse noxious inhibitory controls (DNIC) following nerve injury (Bannister et al., 2015), and intra-RVM injection of lidocaine restored DNIC in the setting of medication-

overuse headache (Okada-Ogawa et al., 2009). Further studies measuring forepaw hyperalgesia are needed to test the hypothesis that 5-HT_3R signaling maintains widespread latent sensitization of post-surgical pain.

The RVM 5-HT neuron → spinal 5-HT_3R pathway is just one of many descending pain facilitatory mechanisms (Millan, 2002). Others include descending GABAergic disinhibition (François et al., 2017) and α_{1A}R-mediated noradrenergic pronociceptive signaling (Taylor and Westlund, 2017; Kohro et al., 2020). Future studies are needed to determine the contribution of these systems to LS.

Spinal 5-HT_{2A} receptors do not contribute to latent sensitization of post-surgical pain.

The 5-HT_{2A}R antagonist MDL-11,939 did not change NTX-induced reinstatement of mechanical or heat hypersensitivity when tested 3 weeks after plantar incision, consistent with the lack of effect of the 5-HT_{2A}R antagonist ketanserin on noxious mechanical or heat stimulus-evoked firing of hypothalamic wide dynamic range neurons in normal or neuropathic rats (Patel and Dickenson, 2018). By contrast, others report that intrathecal injection of 5-HT_{2A} receptor antagonists blocked mechanical hypersensitivity, thermal hypersensitivity and/or dorsal horn neuronal firing in models of trigeminal nerve injury (Okubo et al., 2013), chemotherapeutic drug administration (Thibault et al., 2008), HIV (Van Steenwinckel et al., 2008) or facial inflammation (Alba-Delgado et al., 2018). Thus, the contribution of spinal 5-HT_{2A}R signaling may depend on the type (neuropathic vs inflammatory) and duration (hours vs weeks) of the model, as well as modality of hypersensitivity. We conclude that spinal 5-HT_{2A} receptors do not contribute to long-lasting post-surgical latent pain sensitization.

Incision establishes μ-opioid receptor constitutive activity (MOR_{CA}) in the RVM

We report here that microinjection of CTAP into the RVM reinstated hypersensitivity. Our data are consistent with Porreca and colleagues who reported that a subset of rats displayed no pain-like behavior following spinal nerve ligation, and in these animals, intra-RVM lidocaine induced mechanical hypersensitivity; i.e., inhibition of inhibitory RVM signaling unmasked hypersensitivity during latent sensitization (De Felice et al., 2011). We conclude that injury engages endogenous inhibitory MOR activity within the RVM to maintain LS in a state of remission. This MOR activity could be driven by a ligand-dependent mechanism involving tonic opioid release. Indeed, endogenous opioid peptide signaling in the RVM is integral to the descending inhibitory control of transient nociception. For example, RVM injection of naltrexone blocks the antinociception produced by intra-PAG microinjection of morphine (Kiefel et al., 1993). However, the contribution of endogenous opioidergic mechanisms in the RVM towards the control of injury-induced hyperalgesia is much less clear. For example, MOR signaling in the RVM might not contribute to hyperalgesia in the CFA model of inflammatory pain (Hurley

and Hammond, 2001). Here, in the setting of incision, we present two key pieces of data that promote the idea that MOR_{CA}, rather than opioid release, tonically inhibits post-surgical pain. First, intra-RVM administration of 6β-naltrexol (a neutral opioid receptor antagonist with no intrinsic activity) did not reinstate hypersensitivity. Second, co-administration of 6β-naltrexol prevented CTAP-induced reinstatement of hypersensitivity, arguing that CTAP acts as an inverse agonist with intrinsic activity at MOR. Further ruling out a contribution of endogenous opioids comes from studies in opioid peptide knockout mice (Walwyn et al., 2016). Germline deletion of pro-enkephalin, pro-endorphin or pro-dynorphin did not prevent the reinstatement of hypersensitivity that was triggered by systemic blockade of opioid receptors with the CNS-penetrant naloxone. We conclude that injury triggers MOR_{CA} not only at the dorsal horn of the spinal cord as previously described (Corder et al., 2013; Walwyn et al., 2016), but also at the RVM.

Our use of *in vivo* brain or intrathecal microinjections precludes the knowledge of opioid or 5-HT_3 receptor antagonist concentrations at their receptors. As a result, and given that concentrations of compounds were several times their IC_{50} in the injection solution, it is possible that non-specific receptor activation may have contributed to our observed behavioral effects, and our results should be interpreted with this in mind. However, CTAP, ondansetron and MDL-11,939 are potent, selective antagonists of MOR (Kramer et al., 1989), 5-HT_3 (Thompson and Lummis, 2006) and 5-HT_{2A}Rs (Pehek et al., 2006) respectively.

Conclusion

As schematized in Figure 5, we conclude that plantar incision establishes acute hypersensitivity that gradually resolves over 3 weeks but is replaced by a latent sensitization that is tonically masked by MOR_{CA} in the RVM. Latent post-surgical pain can be revealed by administering opioid receptor inverse agonists. Further RVM chemogenetic and intrathecal pharmacology studies then revealed that a bilateral descending serotonergic facilitatory pathway mediates LS and is recruited to induce mechanical and thermal hypersensitivity. This may have translational significance as clinical trials indicate that NTX-induced hypersensitivity might develop in humans (Pereira et al., 2015; Springborg et al., 2020), and could conceivably contribute to episodic hyperalgesia following disruption of endogenous opioid receptor activity such as occurs during stress (Taylor and Corder, 2014), and generalized pain syndromes such as fibromyalgia and irritable bowel syndrome (Reichling and Levine, 2009). 5-HT_3R antagonists have yielded disappointing results in clinical trials for *neuropathic* pain states (McCleane et al., 2003; Tuveson et al., 2011) possibly due to a lack of CNS availability following i.v. administration (Chiang et al., 2021). However, if further research indicates that LS contributes to the pathogenesis of chronic pain states, then this would encourage future studies to determine whether 5-HT_3R antagonists might be utilized as pharmacotherapy for chronic *inflammatory* pain states that rely on LS.

Author contributions

Conceptualization: A.H.C., N.S.H. and B.K.T.; *Statistical analysis:* A.H.C.; *Funding acquisition:* B.K.T.; *Experimental Investigation:* A.H.C., N.S.H. and P.P.; *Supervision:* B.K.T.; *Visualization:* A.H.C. and N.S.H.; *Writing – original draft:* A.H.C. and N.S.H.; *Writing – review & editing:* A.H.C., N.S.H. and B.K.T.

References

Alba-Delgado C, Mountadem S, Mermet-Joret N, Monconduit L, Dallel R, Artola A, Antri M (2018) 5-HT 2A receptor-induced morphological reorganization of PKCγ-expressing interneurons gates inflammatory mechanical allodynia in rat. J Neurosci 38:10489–10504.

Bannister K, Patel R, Goncalves L, Townson L, Dickenson AH (2015) Diffuse noxious inhibitory controls and nerve injury: Restoring an imbalance between descending monoamine inhibitions and facilitations. Pain 156:1803–1811.

Basu P, Custodio-Patsey L, Prasoon P, Smith BN, Taylor BK (2021) Sex differences in protein kinase A signaling of the latent postoperative pain sensitization that is masked by kappa opioid receptors in the spinal cord. J Neurosci:JN-RM-2622-20.

Bee LA, Dickenson AH (2008) Descending facilitation from the brainstem determines behavioural and neuronal hypersensitivity following nerve injury and efficacy of pregabalin. Pain 140:209–223.

Bowker RM, Westlund KN, Coulter JD (1981) Origins of serotonergic projections to the spinal cord in rat: an immunocytochemical-retrograde transport study. Brain Res 226:187–199.

Bullitt E (1990) Expression of c-fos-like protein as a marker for neuronal activity following noxious stimulation in the rat. J Comp Neurol 296:517–530.

Cai YQ, Wang W, Hou YY, Pan ZZ (2014) Optogenetic activation of brainstem serotonergic neurons induces persistent pain sensitization. Mol Pain 10:70.

Carr FB, Géranton SM, Hunt SP (2014) Descending controls modulate inflammatory joint pain and regulate CXC chemokine and iNOS expression in the dorsal horn. Mol Pain 10:1–14.

Chang EY, Chen X, Sandhu A, Li CY, Luo ZD (2013) Spinal 5-HT3 receptors facilitate behavioural hypersensitivity induced by elevated calcium channel alpha-2-delta-1 protein. Eur J Pain (United Kingdom) 17:505–513.

Chaplan SR, Bach FW, Pogrel JW, Chung JM, Yaksh TL (1994) Quantitative assessment of tactile allodynia in the rat paw. J

Neurosci Methods.

Chen QL, Heinricher MM (2019) Descending Control Mechanisms and Chronic Pain. Curr Rheumatol Rep 21:1–7.

Chiang MD, Frey K, Lee C, Kharasch ED, Tallchief D, Sawyer C, Blood J, Back H, Kagan L, Haroutounian S (2021) Plasma and cerebrospinal fluid pharmacokinetics of ondansetron in humans. Br J Clin Pharmacol 87:516–526.

Cleary DR, Heinricher MM (2013) Adaptations in responsiveness of brainstem pain-modulating neurons in acute compared with chronic inflammation. Pain 154:845–855.

Cooper AH, Hedden NS, Corder G, Lamerand SR, Donahue RR, Morales-Medina JC, Selan L, Prasoon P, Taylor BK (2021) Endogenous mu opioid receptor activity in the lateral and capsular subdivisions of the right central nucleus of the amygdala prevents chronic postoperative pain. J Neurosci Res (In Press).

Corder G, Doolen S, Donahue RR, Winter MK, Jutras BL, He Y, Hu X, Wieskopf JS, Mogil JS, Storm DR, Wang ZJ, McCarson KE, Taylor BK (2013) Constitutive μ-opioid receptor activity leads to long-term endogenous analgesia and dependence. Science (80-) 341.

Custodio-Patsey L, Donahue RRRR, Fu W, Lambert J, Smith BNBN, Taylor BK (2020) Sex differences in kappa opioid receptor inhibition of latent postoperative pain sensitization in dorsal horn. Neuropharmacology 163:107726.

De Felice M, Sanoja R, Wang R, Vera-Portocarrero L, Oyarzo J, King T, Ossipov MH, Vanderah TW, Lai J, Dussor GO, Fields HL, Price TJ, Porreca F (2011) Engagement of descending inhibition from the rostral ventromedial medulla protects against chronic neuropathic pain. Pain 152:2701–2709

Dixon WJ (1965) The Up-and-Down Method for Small Samples. J Am Stat Assoc 60:967–978.

Dogrul A, Ossipov MH, Porreca F (2009) Differential mediation of descending pain facilitation and inhibition by spinal 5HT-3 and 5HT-7 receptors. Brain Res 1280:52–59.

Fields H (2004) State-dependent opioid control of pain. Nat Rev Neurosci 5:565–575.

Fields HL (1992) Is there a facilitating component to central pain modulation? APS J 1:71–78.

Fields HL, Bry J, Hentall I, Zorman G (1983) The activity of neurons in the rostral medulla of the rat during withdrawal from noxious heat. J Neurosci 3:2545–2552.

François A, Low SA, Sypek EI, Christensen AJ, Sotoudeh C, Beier KT, Ramakrishnan C, Ritola KD, Sharif-Naeini R, Deisseroth K, Delp SL, Malenka RC, Luo L, Hantman AW, Scherrer G (2017) A Brainstem-Spinal Cord Inhibitory Circuit for Mechanical Pain Modulation by GABA and Enkephalins. Neuron 93.

Fu W, Nelson TS, Santos DFDF, Doolen S, Gutierrez JJPJJP, Ye N, Zhou J, K. Taylor B, Taylor BK (2019) An NPY Y1 receptor antagonist unmasks latent sensitization and reveals the contribution of protein kinase A and Epac to chronic

565 inflammatory pain. 160:1754–1765.

566 Fu W, Wessel CR, Taylor BK (2020) Neuropeptide Y tonically inhibits an NMDAR➔AC1➔TRPA1/TRPV1 mechanism of the
567 affective dimension of chronic neuropathic pain. Neuropeptides 80:102024.

568 Gao K, Mason P (2000) Serotonergic Raphe Magnus Cells That Respond to Noxious Tail Heat Are Not ON or OFF cells. J
569 Neurophysiol 84:1719–1725.

570 Glare P, Aubrey KR, Myles PS (2019) Transition from acute to chronic pain after surgery. Lancet 393:1537–1546.

571 Guillery RW (2002) On counting and counting errors. J Comp Neurol 447:1–7.

572 Hargreaves K, Dubner R, Brown F, Flores C, Joris J (1988) A new and sensitive method for measuring thermal nociception in
573 cutaneous hyperalgesia. Pain 32:77–88.

574 Heinricher MM (2016) Pain Modulation and the Transition from Acute to Chronic Pain. Adv Exp Med Biol 904:105–115.

575 Heinricher MM, Barbaro NM, Fields HL (1989) Putative Nociceptive Modulating Neurons in the Rostral Ventromedial
576 Medulla of the Rat: Firing of On- and Off-Cells Is Related to Nociceptive Responsiveness. Somatosens Mot Res 6:427–
577 439.

578 Heinricher MM, Morgan MM, Fields HL (1992) Direct and indirect actions of morphine on medullary neurons that modulate
579 nociception. Neuroscience 48:533–543.

580 Heinricher MM, Tavares I, Leith JL, Lumb BM (2009) Descending control of nociception: Specificity, recruitment and
581 plasticity. Brain Res Rev 60:214–225

582 Hurley RW, Hammond DL (2001) Contribution of endogenous enkephalins to the enhanced analgesic effects of supraspinal
583 mu opioid receptor agonists after inflammatory injury. J Neurosci 21:2536–2545.

584 Khasabov SG, Malecha P, Noack J, Tabakov J, Giesler GJ, Simone DA (2017) Hyperalgesia and sensitization of dorsal horn
585 neurons following activation of NK-1 receptors in the rostral ventromedial medulla. J Neurophysiol:jn.00478.2017.

586 Kiefel JM, Rossi GC, Bodnar RJ (1993) Medullary μ and δ opioid receptors modulate mesencephalic morphine analgesia in
587 rats. Brain Res 624:151–161.

588 Kim YS, Chu Y, Han L, Li M, Li Z, LaVinka PC, Sun S, Tang Z, Park K, Caterina MJ, Ren K, Dubner R, Wei F, Dong X (2014)
589 Central terminal sensitization of TRPV1 by descending serotonergic facilitation modulates chronic pain. Neuron
590 81:873–887.

591 Kincaid W, Neubert MJ, Xu M, Kim CJ, Heinricher MM (2006) Role for medullary pain facilitating neurons in secondary
592 thermal hyperalgesia. J Neurophysiol 95:33–41.

593 King T, Vera-Portocarrero L, Gutierrez T, Vanderah TW, Dussor G, Lai J, Fields HL, Porreca F (2009) Unmasking the tonic-

aversive state in neuropathic pain. Nat Neurosci 12:1364–1366.

Kohro Y et al. (2020) Spinal astrocytes in superficial laminae gate brainstem descending control of mechanosensory hypersensitivity. Nat Neurosci 23:1376–1387.

Kramer TH, Shook JE, Kazmierski W, Ayres EA, Wire WS, Hruby VJ, Burks TF (1989) Novel peptidic Mu opioid antagonists: Pharmacologic characterization in vitro and in vivo. J Pharmacol Exp Ther 249:544–551.

Krashes MJ, Koda S, Ye CP, Rogan SC, Adams AC, Cusher DS, Maratos-Flier E, Roth BL, Lowell BB (2011) Rapid, reversible activation of AgRP neurons drives feeding behavior in mice. J Clin Invest 121:1424–1428.

LaGraize SC, Guo W, Yang K, Wei F, Ren K, Dubner R (2010) Spinal cord mechanisms mediating behavioral hyperalgesia induced by neurokinin-1 tachykinin receptor activation in the rostral ventromedial medulla. Neuroscience 171:1341–1356.

Lam H, Maga M, Pradhan A, Evans CJ, Maidment NT, Hales TG, Walwyn W (2011) Analgesic tone conferred by constitutively active mu opioid receptors in mice lacking β-arrestin 2. Mol Pain 7:24.

Madisen L, Zwingman TA, Sunkin SM, Oh SW, Zariwala HA, Gu H, Ng LL, Palmiter RD, Hawrylycz MJ, Jones AR, Lein ES, Zeng H (2010) A robust and high-throughput Cre reporting and characterization system for the whole mouse brain. Nat Neurosci 13:133–140.

Manvich DF, Webster KA, Foster SL, Farrell MS, Ritchie JC, Porter JH, Weinshenker D (2018) The DREADD agonist clozapine N-oxide (CNO) is reverse-metabolized to clozapine and produces clozapine-like interoceptive stimulus effects in rats and mice. Sci Rep 8:1–10.

McCleane GJ, Suzuki R, Dickenson AH (2003) Does a Single Intravenous Injection of the 5HT3 Receptor Antagonist Ondansetron Have an Analgesic Effect in Neuropathic Pain? A Double-Blinded, Placebo-Controlled Cross-Over Study. Anesth Analg 97:1474–1478.

Millan MJ (2002) Descending control of pain. Prog Neurobiol 66:355–474.

Njoo C, Heinl C, Kuner R (2014) In vivo siRNA transfection and gene knockdown in spinal cord via rapid noninvasive lumbar intrathecal injections in mice. J Vis Exp:1–4.

Okubo M, Castro A, Guo W, Zou S, Ren K, Wei F, Keller A, Dubner R (2013) Transition to Persistent Orofacial Pain after Nerve Injury Involves Supraspinal Serotonin Mechanisms. 33:5152–5161.

Patel R, Dickenson AH (2018) Modality selective roles of pro-nociceptive spinal 5-HT2A and 5-HT3 receptors in normal and neuropathic states. Neuropharmacology 143:29–37.

Paxinos G, Franklin KBJ (2013) The Mouse Brain in Stereotaxic Coordinates, 4th Ed. London, UK: Academic Press.

623 Pehek EA, Nocjar C, Roth BL, Byrd TA, Mabrouk OS (2006) Evidence for the Preferential Involvement of 5-HT2A Serotonin
624 Receptors in Stress- and Drug-Induced Dopamine Release in the Rat Medial Prefrontal Cortex. :265–277.

625 Peirs C, Williams SPG, Zhao X, Walsh CE, Gedeon JY, Cagle NE, Goldring AC, Hioki H, Liu Z, Marell PS, Seal RP (2015) Dorsal
626 Horn Circuits for Persistent Mechanical Pain. Neuron 87:797–812.

627 Pereira MP, Donahue RR, Dahl JB, Werner M, Taylor BK, Werner MU (2015) Endogenous opioid-masked latent pain
628 sensitization: Studies from mouse to human. PLoS One 10.

629 Pogatzki EM, Raja SN (2003) A mouse model of incisional pain. Anesthesiology 99:1023–1027.

630 Porreca F, Ossipov MH, Gebhart GF (2002) Chronic pain and medullary descending facilitation. Trends Neurosci.

631 Potrebic SB, Fields HL, Mason P (1994) Serotonin immunoreactivity is contained in one physiological cell class in the rat
632 rostral ventromedial medulla. J Neurosci 14:1655–1665.

633 Raehal KM (2005) In Vivo Characterization of 6 -Naltrexol, an Opioid Ligand with Less Inverse Agonist Activity Compared
634 with Naltrexone and Naloxone in Opioid-Dependent Mice. J Pharmacol Exp Ther 313:1150–1162.

635 Rahman W, Suzuki R, Rygh LJ, Dickenson AH (2004) Descending serotonergic facilitation mediated through rat spinal 5HT3
636 receptors is unaltered following carrageenan inflammation. Neurosci Lett 361:229–231.

637 Reichling DB, Levine JD (2009) Critical role of nociceptor plasticity in chronic pain. Trends Neurosci 32:611–618.

638 Ren K, Dubner R (2002) Descending modulation in persistent pain: An update. Pain 100:1–6.

639 Sally EJ, Xu H, Dersch CM, Hsin L-W, Chang L-T, Prisinzano TE, Simpson DS, Giuvelis D, Rice KC, Jacobson AE, Cheng K, Bilsky
640 EJ, Rothman RB (2010) Identification of a novel â€œalmost neutralâ€ Î¼-opioid receptor
641 antagonist in CHO cells expressing the cloned human Î¼-opioid receptor. Synapse 64:280–288.

642 Scott MM, Wylie CJ, Lerch JK, Murphy R, Lobur K, Herlitze S, Jiang W, Conlon RA, Strowbridge BW, Deneris ES (2005) A
643 genetic approach to access serotonin neurons for in vivo and in vitro studies. Proc Natl Acad Sci U S A 102:16472–
644 16477.

645 Sikandar S, Bannister K, Dickenson AH (2012) Brainstem facilitations and descending serotonergic controls contribute to
646 visceral nociception but not pregabalin analgesia in rats. Neurosci Lett 519:31–36.

647 Sirohi S, Dighe S V, Madia PA, Yoburn BC (2009) The relative potency of inverse opioid agonists and a neutral opioid
648 antagonist in precipitated withdrawal and antagonism of analgesia and toxicity. J Pharmacol Exp Ther 330:513–519.

649 Skagerberg G, Björklund A (1985) Topographic principles in the spinal projections of serotonergic and non-serotonergic
650 brainstem neurons in the rat. Neuroscience 15:445–480.

651 Snyder LM et al. (2018) Kappa Opioid Receptor Distribution and Function in Primary Afferents Article Kappa Opioid

652 Receptor Distribution and Function in Primary Afferents. Neuron 99:1274-1288.e6.

653 Springborg AD, Jensen EK, Kreilgaard M, Petersen MA, Papathanasiou T, Lund TM, Taylor BK, Werner MU (2020) High-dose
654 naloxone: Effects by late administration on pain and hyperalgesia following a human heat injury model. A
655 randomized, double-blind, placebo-controlled, crossover trial with an enriched enrollment design. PLoS One 15:1–22.

656 Steenwinckel J Van, Brisorgueil M, Fischer J, Gingrich JA, Bourgoin S, Hamon M, Bernard R, Conrath M (2008) Role of spinal
657 serotonin 5-HT2A receptor in 2 0 , 3 0 -dideoxycytidine- induced neuropathic pain in the rat and the mouse. 137:66–
658 80.

659 Suzuki R, Rahman W, Hunt SP, Dickenson AH (2004) Descending facilitatory control of mechanically evoked responses is
660 enhanced in deep dorsal horn neurones following peripheral nerve injury. Brain Res 1019:68–76.

661 Taylor BK, Basbaum AI (1995) Neurochemical Characterization of Extracellular Serotonin in the Rostral Ventromedial
662 Medulla and Its Modulation by Noxious Stimuli. J Neurochem 65:578–589.

663 Taylor BK, Corder G (2014) Endogenous analgesia, dependence, and latent pain sensitization.

664 Taylor BK, Westlund KN (2017) The noradrenergic locus coeruleus as a chronic pain generator. J Neurosci Res 95:1336–
665 1346.

666 Thibault K, Van Steenwinckel J, Brisorgueil MJ, Fischer J, Hamon M, Calvino B, Conrath M (2008) Serotonin 5-HT2A receptor
667 involvement and Fos expression at the spinal level in vincristine-induced neuropathy in the rat. Pain 140:305–322.

668 Thompson AJ, Lummis SCR (2006) 5-HT3 receptors. Curr Pharm Des 12:3615–3630.

669 Tillu D V, Gebhart GF, Sluka KA (2008) Descending facilitatory pathways from the RVM initiate and maintain bilateral
670 hyperalgesia after muscle insult. Pain 136:331–339.

671 Tuveson B, Leffler AS, Hansson P (2011) Ondansetron, a 5HT3-antagonist, does not alter dynamic mechanical allodynia or
672 spontaneous ongoing pain in peripheral neuropathy. Clin J Pain 27:323–329.

673 Urban MO, Jiang MC, Gebhart GF (1996) Participation of central descending nociceptive facilitatory systems in secondary
674 hyperalgesia produced by mustard oil. Brain Res 737:83–91.

675 Van Steenwinckel J, Brisorgueil MJ, Fischer J, Vergé D, Gingrich JA, Bourgoin S, Hamon M, Bernard R, Conrath M (2008) Role
676 of spinal serotonin 5-HT2A receptor in 2',3'-dideoxycytidine-induced neuropathic pain in the rat and the mouse. Pain
677 137:66–80.

678 Vera-Portocarrero LP, Zhang ET, Ossipov MH, Xie JY, King T, Lai J, Porreca F (2006) Descending facilitation from the rostral
679 ventromedial medulla maintains nerve injury-induced central sensitization. Neuroscience 140:1311–1320.

680 Walwyn WM, Chen W, Kim H, Minasyan A, Ennes HS, McRoberts JA, Marvizón JCG (2016) Sustained Suppression of

681 Hyperalgesia during Latent Sensitization by μ-, δ-, and κ-opioid receptors and α2A Adrenergic Receptors: Role of
682 Constitutive Activity. J Neurosci 36:204–221.

683 Wang R, King T, De Felice M, Guo W, Ossipov MH, Porreca F (2013) Descending facilitation maintains long-term
684 spontaneous neuropathic pain. J Pain 14:845–853.

685 Wang Z, Jiang C, Yao H, Chen O, Rahman S, Gu Y, Zhao J, Huh Y, Ji RR (2021) Central opioid receptors mediate morphine-
686 induced itch and chronic itch via disinhibition. Brain 144:665–681.

687 Wei F, Dubner R, Zou S, Ren K, Bai G, Wei D, Guo W (2010) Molecular Depletion of Descending Serotonin Unmasks Its Novel
688 Facilitatory Role in the Development of Persistent Pain. 30:8624–8636.

689 Zeitz KP, Guy N, Malmberg AB, Dirajlal S, Martin WJ, Sun L, Bonhaus DW, Stucky CL, Julius D, Basbaum AI (2002) The 5-HT3
690 subtype of serotonin receptor contributes to nociceptive processing via a novel subset of myelinated and
691 unmyelinated nociceptors. J Neurosci 22:1010–1019.

Figures

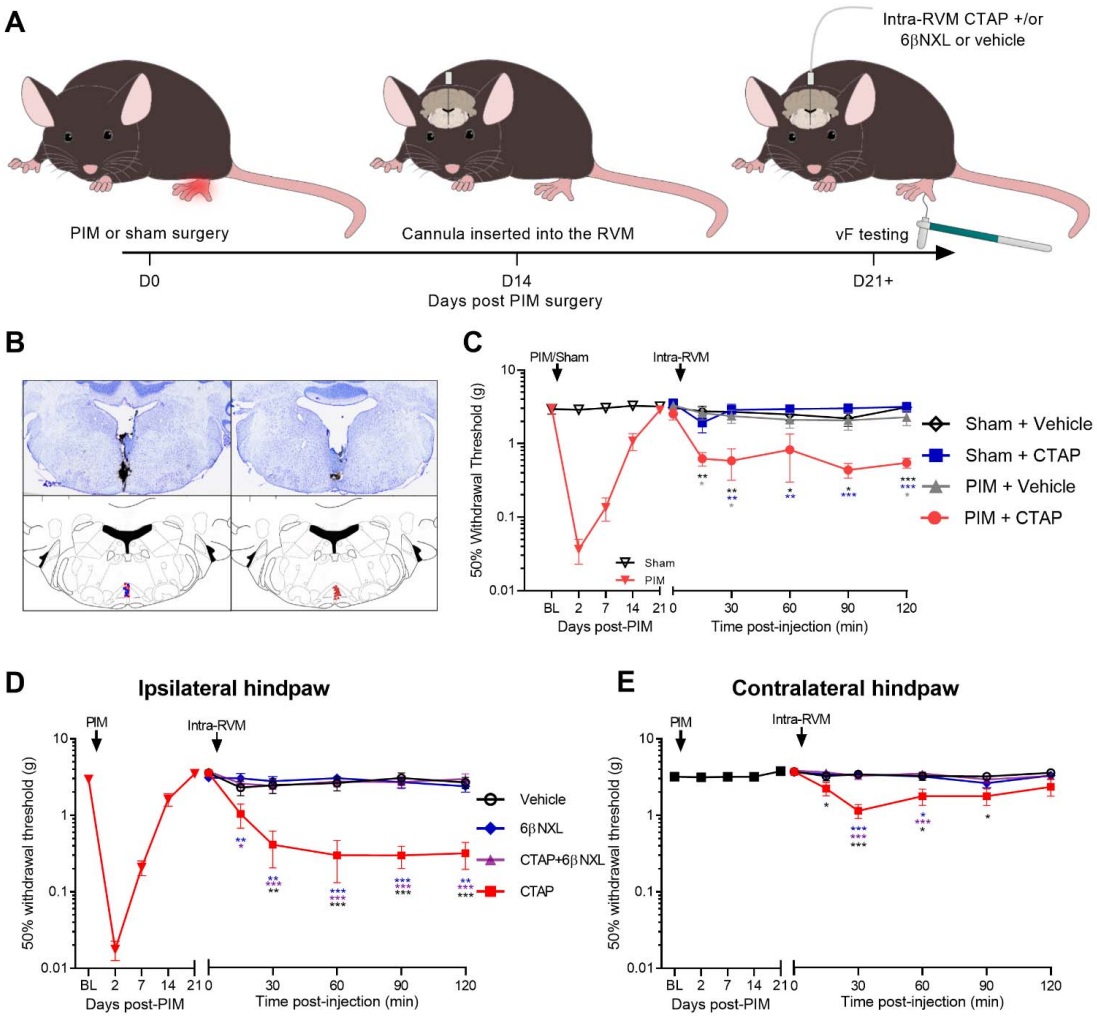

Figure 1 - MOR constitutive activity (MOR_{CA}) in the RVM maintains LS in remission.

(A) Schematic illustration representing the timeline of experimental procedures. **(B)** Representative section with post-mortem India ink injection *(top)*; location of injection sites in the RVM *(bottom)* for experiments shown in **C** *(left)* and **D-E** *(right)*. **(C)** Mechanical thresholds at the ipsilateral hindpaw following PIM or sham surgery *(left)*, and following resolution of PIM-induced hypersensitivity, intra-RVM injection of the MOR inverse agonist CTAP (0.3 µg/0.25 µL) or vehicle (saline) (*right*; *n* = 7). **(D-E)** Mechanical thresholds at the ipsilateral **(D)** and contralateral **(E)** hindpaw over 21 days following incision *(left)* and after intra-RVM injection (*right*) of CTAP (0.3 µg/0.25 µL), the neutral opioid antagonist 6β-naltrexol (3 µg/0.25 µL), both CTAP and 6β-naltrexol, or vehicle (10% DMSO in saline) (*n* = 8). 2-way RM ANOVAs with Bonferroni post-tests: * $P < 0.05$; ** $P < 0.01$; *** $P < 0.001$.

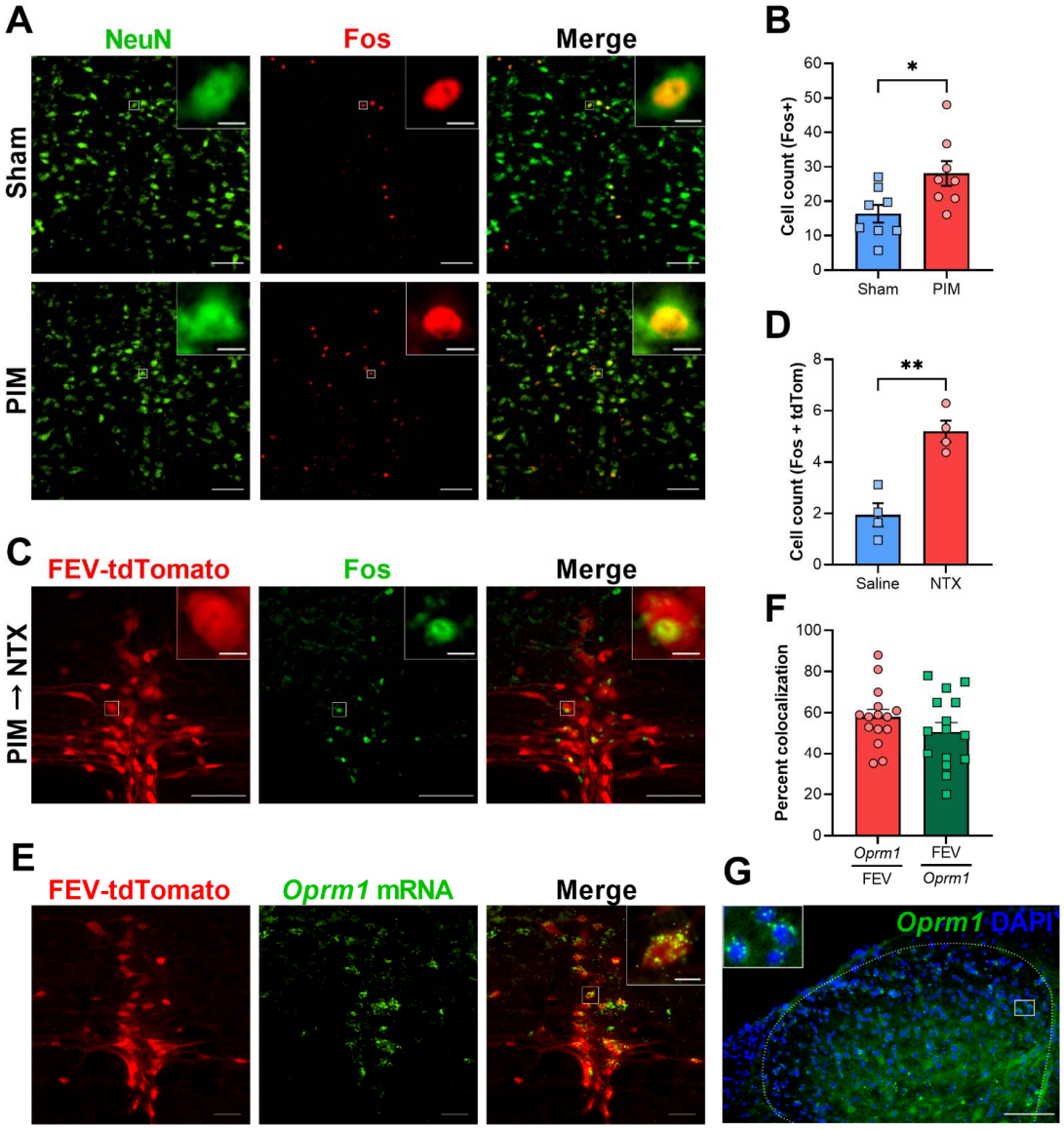

Figure 2 – Increased Fos expression in medullary raphe 5-HT neurons during NTX-induced reinstatement of hyperalgesia. **(A)** Representative images demonstrate co-localization in the RMg and RPa of NeuN (green) and Fos (red) immunofluorescence 21 days after PIM (30 Fos+, NeuN+ cells) or Sham (9 Fos+, NeuN+ cells) surgery. No NeuN-negative, Fos+ neurons were observed. Scale bars = 100 µm; inset = 10 µm. **(B)** Quantification of Fos+ (red) cells in the RMg and RPa. PIM increased RMg and RPa Fos expression compared with sham-operated mice (Unpaired t-test; * $P < 0.05$; n = 8 mice, 5 to 6 sections per mouse). **(C)** Representative images demonstrating FEV-tdTomato (red; 62 cells) and Fos (green; 36 cells) co-localization (6 FEV-tdtomato+, Fos+ cells) in the RMg and RPa 21 days after incision

and 2h after systemic NTX (3 mg/kg) injection. Scale bars = 100 µm; inset = 10 µm; images are maximum intensity projections of 11 z-scans. **(D)** Quantification of cells co-expressing FEV-tdTomato and Fos in the RMg and RPa of male and female FEV^{cre}::Ai14 mice 21 days following incision and 2h after systemic NTX (3 mg/kg) or saline injection (Unpaired t-test; ** $P < 0.01$; $n = 4$ mice, 5 to 6 sections per mouse). **(E)** Representation images of FEV-tdTomato (red) and FISH of *Oprm1* (green) mRNA in the RMg and RPa Scale bars = 50 µm; inset = 10 µm. **(F)** Quantification of percentage colocalization of FEV-tdTomato and *Oprm1* mRNA in the RVM ($n = 15$ sections from 2 mice). (**G**) Representative image of *Oprm1* mRNA in the spinal dorsal horn. Inset are cropped, enlarged images of boxed regions. Extended Data 2-1A illustrate that Fos was colocalized with neuronal nuclei marker NeuN.

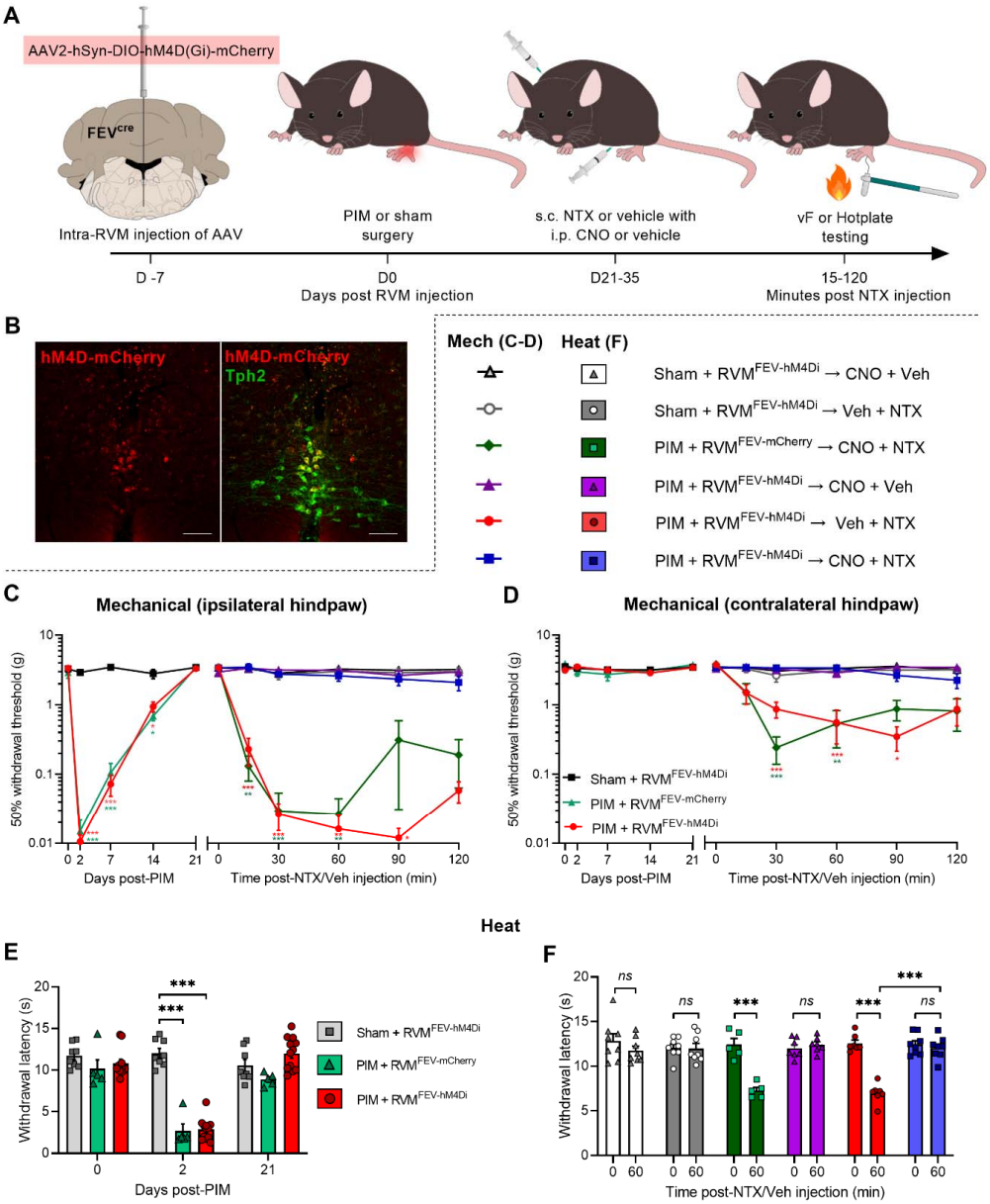

Figure 3 – Chemogenetic inhibition of RVM 5-HT neurons prevents NTX-induced reinstatement of hyperalgesia.

(A) Schematic illustration representing timeline of experimental procedures. FEV^{cre} mice received intra-RVM injection of AAV2-hSyn-DIO-hM4Di-mCherry (RVM$^{FEV\text{-}hM4Di}$) or AAV2-hSyn-DIO-mCherry control (RVM$^{FEV\text{-}mCherry}$). **(B)** Representative image showing colocalization of AAV2-hSyn-DIO-hM4Di-mCherry expression (red) and Tph2 immunofluorescence (green) in

the RVM of FEV^{cre} mice. Scale bars = 100 µm. **(C-D)** Mechanical thresholds at the ipsilateral **(C)** and contralateral **(D)** hindpaws following PIM or sham surgery in FEV^{cre} mice, and effect of CNO or saline administration on NTX-induced reinstatement of mechanical allodynia. PIM-induced hypersensitivity in the ipsilateral hindpaw resolved after 21 days (*Left*; n = 8 (sham) or 12 (PIM) $RVM^{FEV\text{-}hM4Di}$ and 5 $RVM^{FEV\text{-}mCherry}$ controls). CNO prevented NTX-induced reinstatement of hypersensitivity in $RVM^{FEV\text{-}hM4Di}$ mice (*Right; n* = 7-8 $RVM^{FEV\text{-}hM4Di}$, 5 $RVM^{FEV\text{-}mCherry}$ controls). **(E)** Hotplate testing to measure latency of withdrawal in ipsilateral hindpaw 2- and 21-days following PIM or sham surgery (n = 8 (sham) or 12 (PIM) $RVM^{FEV\text{-}hM4Di}$ and 5 $RVM^{FEV\text{-}mCherry}$ controls). **(F)** Hotplate testing to measure the effect of CNO or saline administration on NTX-induced reinstatement of heat allodynia of $RVM^{FEV\text{-}hM4Di}$ mice (n = 7-8 $RVM^{FEV\text{-}hM4Di}$, 5 $RVM^{FEV\text{-}mCherry}$ controls). 2-way RM ANOVAs with Bonferroni post-tests: * $P < 0.05$; ** $P < 0.01$; *** $P < 0.001$.

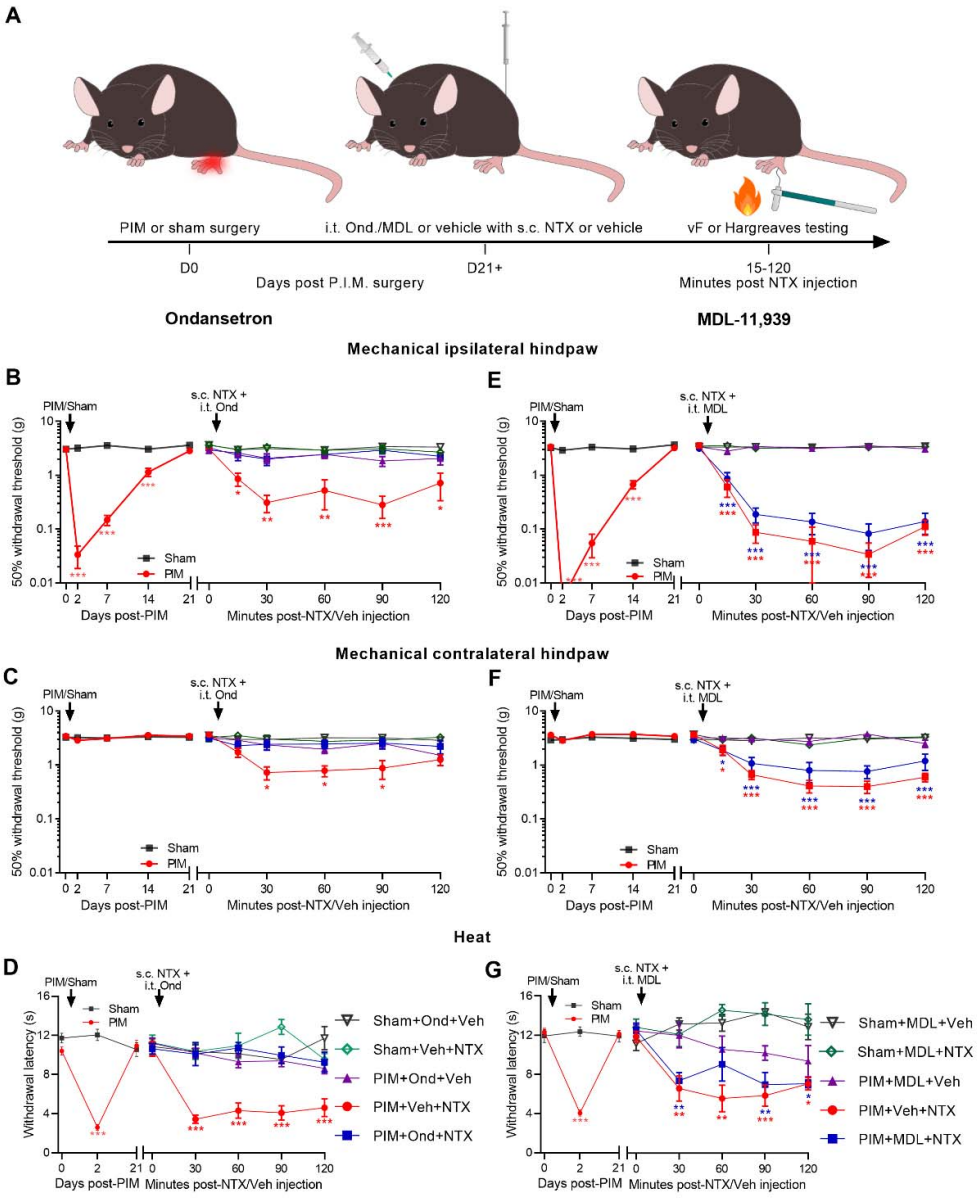

Figure 4 – Spinal 5-HT$_3$Rs but not 5-HT$_{2A}$Rs antagonists prevent NTX-induced reinstatement of mechanical and heat hypersensitivity.

(A) Schematic illustration representing timeline of experimental procedures **(B-C)** Mechanical thresholds at the ipsilateral **(B)** and contralateral **(C)** hindpaws following PIM or sham surgery (*Left*; n = 9 (sham) or 14 (PIM)). Effect of i.t. ondansetron (5-HT$_3$R antagonist) or saline on NTX-induced reinstatement of mechanical allodynia at the ipsilateral **(B)** and contralateral

737 **(C)** hindpaws (*Right*; n = 6-8). **(D)** Hargreaves testing to measure latency of withdrawal in ipsilateral hindpaw 2- and 21-days
738 following PIM or sham surgery (*Left*; *n* = 8 (sham) or 16 (PIM)). Effect of i.t. ondansetron or saline on NTX-induced
739 reinstatement of heat allodynia in ipsilateral hindpaw (*Right*; *n* = 6). **(E-F)** Progression of mechanical allodynia at the
740 ipsilateral **(E)** and contralateral **(F)** hindpaw following PIM or sham surgery (*Left*; *n* = 15). Effect of i.t. MDL-11,939 (5-HT_{2A}R
741 antagonist) or saline on NTX-induced reinstatement of mechanical allodynia at the ipsilateral **(E)** and contralateral **(F)**
742 hindpaws (*Right*; n = 8). **(G)** Hargreaves testing to measure latency of withdrawal in ipsilateral hindpaw 2- and 21-days
743 following PIM or sham surgery (*Left*; *n* = 9 (sham) or 20 (PIM)). Effect of i.t. MDL-11,939 or saline on NTX-induced
744 reinstatement of heat allodynia in ipsilateral hindpaw (*Right*; *n* = 5-7). 2-way RM ANOVAs with Bonferroni's post-tests: * P <
745 0.05; ** P < 0.01; *** P < 0.001.

746

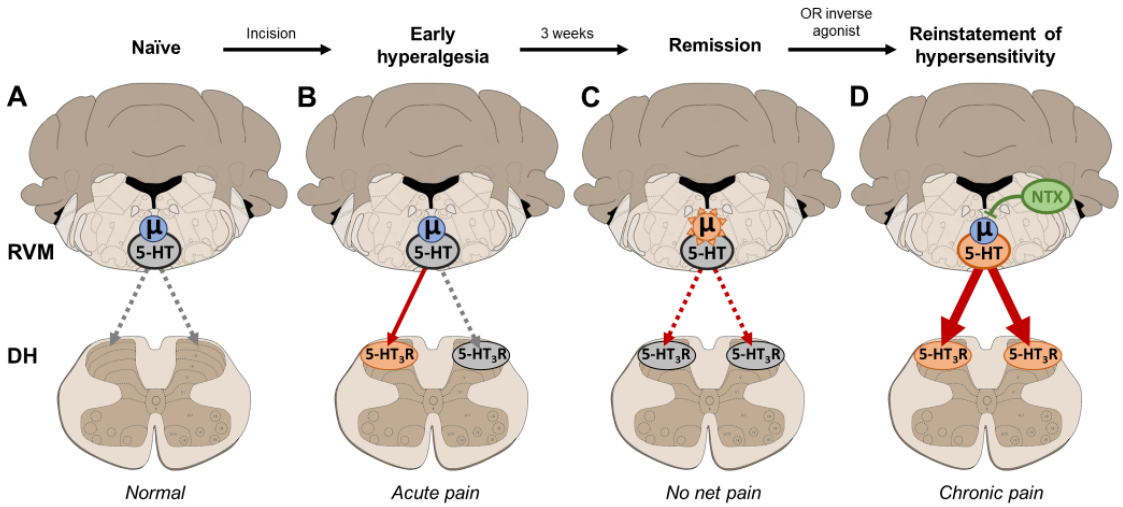

Figure 5 – RVM MOR_{CA} maintains latent pain sensitization in remission.

(A) In the absence of injury, the influence of rostral ventromedial medulla (RVM)-mediated descending serotonergic input to the dorsal horn (DH) is minimal (dotted grey line). **(B)** Soon after injury, descending facilitation of spinal nociceptive processing predominates, leading to unilateral hypersensitivity (red arrow). **(C)** Over time, latent sensitization persists (dotted red line) but is masked and kept in remission by RVM MOR_{CA}. **(D)** Focal or systemic injection of an opioid inverse agonist such as naltrexone (NTX) inhibits MOR_{CA}, unmasking (disinhibiting) descending 5-HT_3 receptor-mediated facilitation, leading to widespread pain reinstatement.

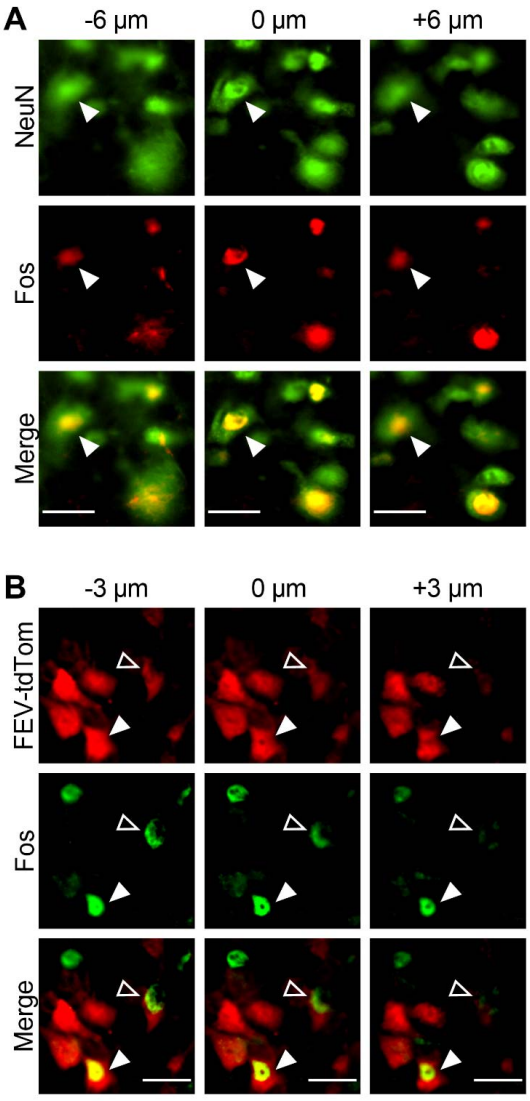

766

767 **Extended Data 2-1 – Colocalization of Fos with NeuN and FEV-tdTomato through the z-axis, Related to Figure**
768 **2.**

769 (A) Co-localization of Fos with NeuN at three z-positions at 6 µm intervals in the RMg. White arrow indicates a neuron
770 positive for both Fos and NeuN immunofluorescence in focus at 0 µm, and out of focus ± 6 µm in the z dimension. (B) Co-
771 localization of Fos with FEV-tdTom at three z-positions at 3 µm intervals in the RMg. White arrow indicates an example of a
772 Fos and FEV-tdTom positive neuron in focus at 0 µm, and out of focus ± 3 µm in the z dimension. Open arrow indicates a

773 Fos-positive neuron in focus at -3 µm, but without FEV-tdTom fluorescence definitively surrounding the nucleus in the same
774 focal plane, thus classified as FEV-tdTom negative. Scale bars = 25 µm